Molecular Mechanics Studies on the Conformations of 2′,3′-Dideoxy-2′,3′-Didehydroguanine Nucleoside, D4G

Shashidhar N. Rao
Searle Research and Development, Skokie, Illinois 60077 USA

ABSTRACT Conformational energy calculations have been presented on guanine nucleoside in which the furanose ring is replaced by 2′,3′-dideoxy-2′,3′-didehydrofuran using molecular mechanics and conformational analysis. Conformational energies have been evaluated using the MM2 and AMBER94 force field parameters at two different dielectric constants. The results are presented in terms of isoenergy contours in the conformational space of the glycosidic (χ) and C4′-C5′ (γ) bonds torsions. In general, the χ-γ interrelationships differ from the corresponding plots for unmodified nucleosides and nucleotides, reported previously. Consistency of the calculated preferred conformations with the x-ray data is sensitive to the force field employed.

INTRODUCTION

Modified nucleosides with both purine and pyrimidine bases have been the subject of many recent investigations as potential antiviral agents (Chu et al., 1988; Dytakina et al., 1994; Andrei et al., 1995; McGuigan et al., 1996a, b; Eriksson et al., 1991; Bolon et al., 1996). In this light, extensive structure-activity relationships (SAR) and pharmacological profiles of modified nucleosides as anti-HIV agents, inhibitors of hepatitis B virus replication, adenylate cyclase inhibitors, antitumor agents, etc. have been reported (Herdewijn et al., 1988; Chu et al., 1989; Robins et al., 1995; Harte et al., 1991; Bhattacharya et al., 1995; Smee et al., 1995). Some modified nucleosides (e.g., 2′,3′-dideoxy-2′,3′-didehydrothymidine; D4T) have unique biological properties rendering them less toxic than AZT and hence viable candidates for clinical trials as anti-HIV agents (Hitchcock, 1991; Genu-Dellac et al., 1991). Pharmacokinetic studies on D4T have shown that this compound is well absorbed and is predominantly eliminated unchanged, in addition to having penetration into the blood-brain barrier in mice (Russell et al., 1989). A few x-ray crystallographic and theoretical studies have been reported on such modified nucleosides (Van Roey and Chu, 1992; Van Roey et al., 1993; O'Leary and Kishi, 1994; Galisteo et al., 1995, 1996; Cody and Kalman, 1992; Everaert et al., 1993a, b; Rao, 1995).

In continuation of a study on the structural and conformational aspects of furanose modified nucleosides (Rao, 1995), this paper has investigated conformational preferences in 2′,3′-dideoxy-2′,3′-didehydroguanidine, D4G. Specifically, molecular mechanics energy evaluation and refinement have been carried out in the conformational space of the glycosidic (χ) and C4′-C5′ (γ) bond torsions using MM2 and AMBER94 force field parameters. In simulations with the MM2 force field, two different charge models were employed, while AMBER94 calculations were carried out using quantum chemically derived charges. The qualitative consistency of the calculated low energy models with the limited single crystal x-ray data on D4G is sensitive to the force field and the charge model used.

METHODS

Preliminary models of **1** (illustrated below schematically) were built using MacroModel (v5.0) and energy refined with the MM2 force field (Mohmadi et al., 1990). The nomenclature adopted for describing the atom names and torsion angles is as described earlier (Rao, 1995; 1998). Multiple conformations of **1** were generated by varying the torsions χ (O1′-C1′-N9-C8) and γ (C3′-C4′-C5′-O5′) (illustrated below) at 10° interval. The resultant collections of 1296 conformations were energy refined using the BatchMin module (Mohamadi et al., 1990) by varying all degrees of freedom except for χ and γ. These torsions were constrained to their starting values with a weight of 1000 kcal/mol-degree. Simulations were carried out using both the MM2 and AMBER94 (Cornell et al., 1995) force fields.

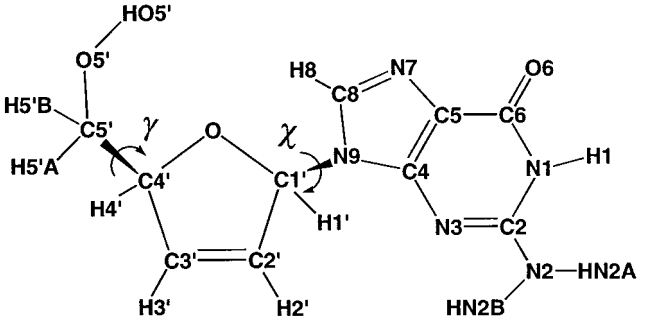

1

In the case of simulations with MM2 force field, two charge models were used. The first one corresponded to partial atomic charges fitted to the quantum chemically derived electrostatic potentials (vide infra), while the second model corresponded to charges derived from the MM2 force field, based on bond dipoles (Mohamadi et al., 1990). The quantum chemically derived partial atomic charges on the atoms of **1** (Appendix) were obtained by fitting to the ab initio electrostatic potential surfaces (calculated using

Received for publication 28 October 1997 and in final form 25 February 1998.

Address reprint requests to Shashidhar N. Rao, Searle Research and Development, 4901 Searle Parkway, Skokie, IL 60077. Tel.: 847-982-4545; Fax: 847-982-4714; E-mail: snrao@ddix4.monsanto.com.

0006-3495/98/06/3131/09 $2.00

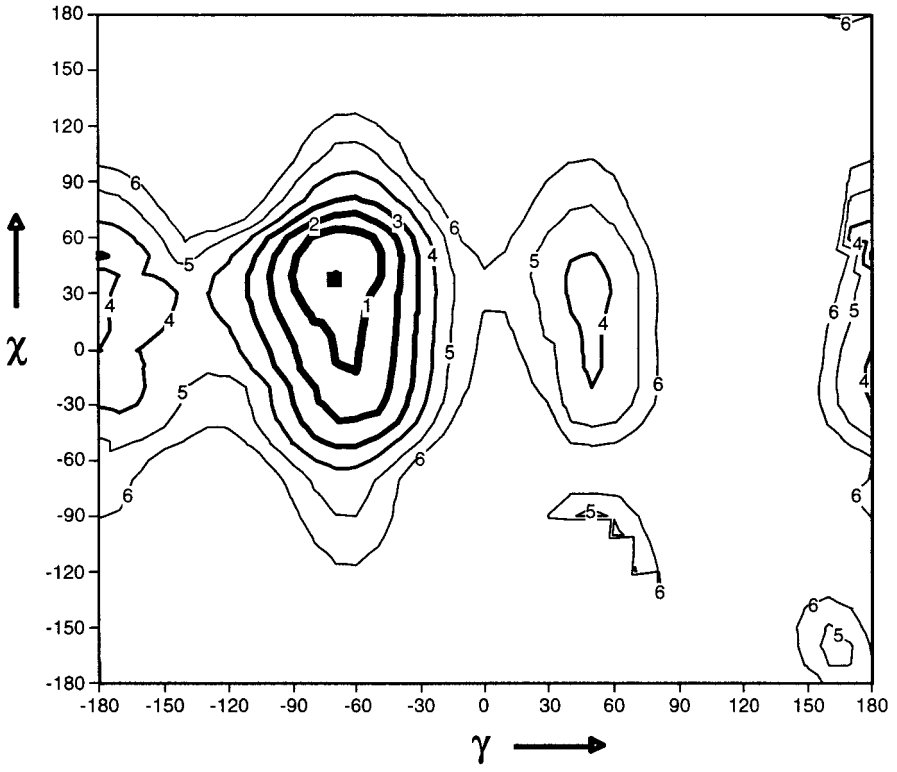

FIGURE 1 Conformational energy map of **1** in the (χ,γ) space (dielectric of 1.0 and MM2 force field). Minima are listed in Table 1.

Gaussian94 (Frisch et al., 1995) with the RHF/6–31G* basis sets). Two values of dielectric, 1 and 4, were employed in the calculations. These dielectric values have been previously used by numerous theoretical investigations on the structure and conformations of nucleic acid constituents and the results obtained therein are qualitatively consistent with experimental data (Saenger, 1984). In addition to the vacuum simulations, calculations have also been carried out using the implicit water solvation model (GBSA) obtained within MacroModel (Mohamadi et al., 1990). These calculations were done using the quantum chemically derived charges at a dielectric of 1.

The results of the conformational energy calculations on **1** are shown in terms of energy plots in the (χ,γ) space, wherein isoenergy contours (1 through 5 kcal/mol) are drawn at 1 kcal/mol intervals (Figs. 1–8). Of these, Figs. 1–4 correspond to energy calculations done with the quantum chemically derived charges, while Figs. 5 and 6 correspond to charges derived from the MM2 force field. Results of calculations incorporating implicit solvation are illustrated in the isoenergy contour plots of Figs. 7 and 8, corresponding to the MM2 and the AMBER94 force fields. In all these plots, the thickest contour corresponds to 1 kcal/mol relative to global minimum and the relative energy value increases as the thickness decreases. Thus the thinnest contour corresponds to 5 kcal/mol. The energy minima are listed in Tables 1–6. Only the global minima are marked by dark solid squares (■) in the (χ,γ) maps.

RESULTS

Fig. 1 illustrates the conformational energy plot of **1** in its (χ,γ) space for the dielectric constant of 1.0 and MM2 force field. The global minimum (M1) is found at (χ,γ) = (40,70°) and corresponds to a structure with *anti* conformation of the base and *gauche*$^-$ conformation about C4′-C5′. The secondary minima obtained in this plot are destabilized by at least 3 kcal/mol (Table 1). Two of these correspond to the *anti* orientation of the base while another to the *syn* orientation of the guanine. The 5 kcal/mol energy contour encloses less than a third of the (χ,γ) space.

By contrast, in Fig. 2, which illustrates the conformational energy plot of **1** for the dielectric constant of 4.0 and MM2 force field, nearly 80% of the (χ,γ) conformational space is enclosed by the 5 kcal/mol energy contour. In this plot, the global minimum at (χ,γ) = (40°,180°) corresponds to a structure with *anti* conformation of the base and *trans* conformation about C4′-C5′. Three secondary minima destabilized by <2 kcal/mol relative to the global minimum are found in the (*anti, gauche*$^-$), (*anti, gauche*$^+$) and (*syn, gauche*$^+$) regions of the (χ,γ) space (Table 2).

The conformational energy plots of **1** corresponding to the AMBER94 force field at the dielectric constants of 1 and 4 are illustrated in Figs. 3 and 4 with their minima listed in Tables 3 and 4. In Fig. 3, the global minimum occurs at (χ,γ) = (220°,50°) and corresponds to the *syn* orientation of the base with a *gauche*$^+$ conformation about C4′-C5′. Only three secondary minima destabilized by >3 kcal/mol (Table

TABLE 1 Energy minima of **1** in the (χ,γ) conformational space (Fig. 1; ϵ = 1; MM2)

Minimum Number	γ (deg)	χ (deg)	Relative Energy (kcal/mol)
1	−70.0	40.0	0.00
2	−170.0	50.0	3.11
3	50.0	30.0	3.75
4	160.0	−160.0	4.72

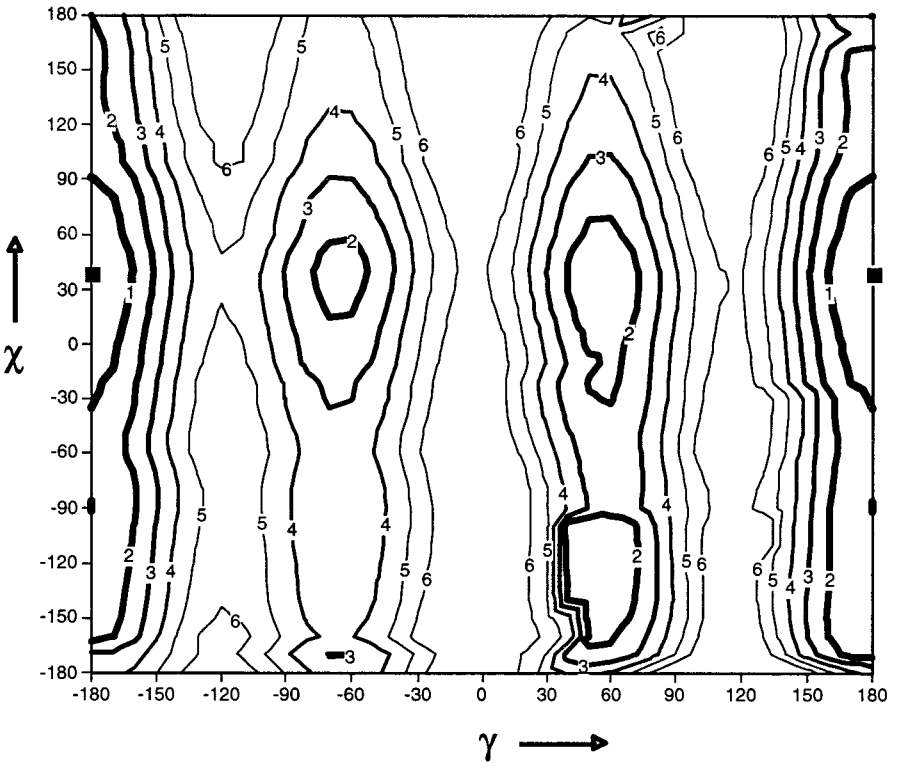

FIGURE 2 Conformational energy map of **1** in the (χ,γ) space (dielectric of 4.0 and MM2 force field). Minima are listed in Table 2.

3) are found in this plot in which <20% of the conformational space is enclosed by the 5 kcal/mol energy contour. As in the case of Fig. 2, this contour encloses a significantly larger part of the conformational space (~60%) in Fig. 4 compared to Fig. 3, where the global minimum still corresponds to the *syn* orientation of the base with a *trans* conformation about C4′-C5′ (Table 4).

The (χ,γ) conformational energy plots in Figs. 5 and 6 corresponding to the dielectric constants of 1 and 4, respectively, and the MM2 charges demonstrate significantly greater degree of flexibility than the plots in Figs. 1 and 2 and are somewhat similar to those in Figs. 3 and 4. The global minimum in Fig. 5 occurs for a high *syn* orientation of the base (Tables 5 and 6). However, conformations corresponding to *anti* orientation of guanine are destabilized by <0.3 kcal/mol relative to the global minimum. Although the positions of the secondary minima correspond to the *syn* orientation of the base (Table 5), numerous conformations with *anti* orientations of the base are feasible in the three standard ranges of the C4′-C5′ torsion. The 5 kcal/mol contour occupies nearly 90% of the total conformational space.

TABLE 2 Energy minima of **1** in the (χ,γ) conformational space (Fig. 2; ϵ = 4; MM2)

Minimum Number	γ (deg)	χ (deg)	Relative Energy (kcal/mol)
1	180.0	40.0	0.00
2	50.0	−100.0	1.01
3	60.0	40.0	1.28
4	−60.0	40.0	1.66

In the (χ,γ) plots computed by including the implicitly GB/SA solvation model (Figs. 7 and 8), the global minima correspond to structures with *anti* orientation of the glycosidic torsion and a *trans* conformation about C4′-C5′. This preference for γ can be rationalized on the basis of the fact that solvation energies are more favorable for extended structures compared to relatively compact structures, as would be obtained with *gauche* conformations. The 5 kcal/mol contours enclosing the global and secondary minima (Tables 7 and 8) cover nearly 70% of the (χ,γ) conformational space. This contrasts significantly with the corresponding coverage in the plots corresponding to calculations without the inclusion of implicit solvation (Figs. 1 and 3).

DISCUSSION

Conformational energy calculations using molecular mechanics methods on D4G have been carried out to understand the energetic preferences of the torsions about the glycosidic and C4′-C5′ bonds. The results demonstrate significant sensitivity to the nature of the force field and the dielectric used in the simulations. Specifically, these factors influence the positions of global minima and the barriers to conformational transitions to secondary minima in the (χ,γ) energy plots. The global minima span four of the possible six conformational combinations of χ and γ, namely (*anti, gauche*$^-$), (*syn, gauche*$^+$), (*anti, trans*) and (*syn, trans*), depending upon the force field and dielectric model used.

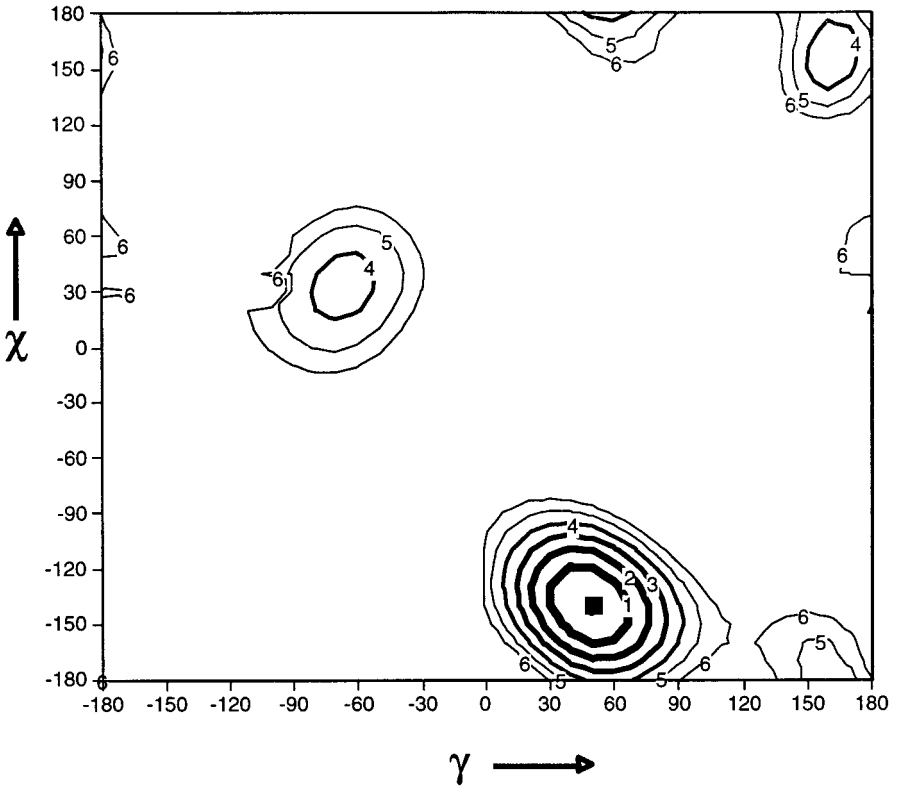

FIGURE 3 Conformational energy map of **1** in the (χ,γ) space (dielectric of 1.0 and AMBER94 force field). Minima are listed in Table 3.

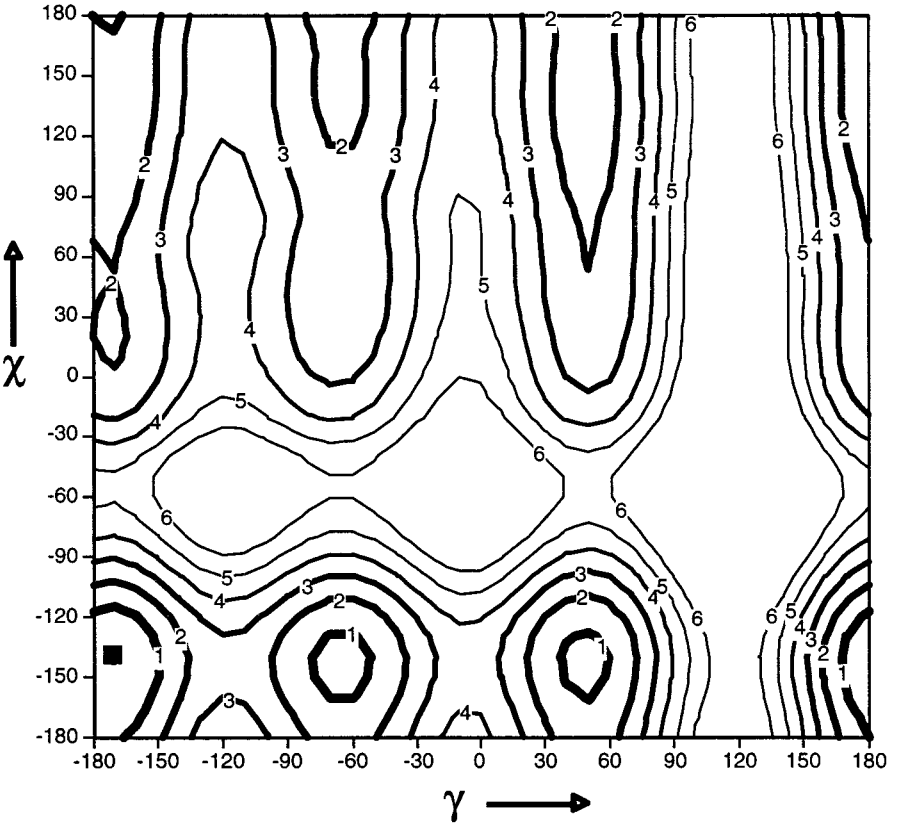

FIGURE 4 Conformational energy map of **1** in the (χ,γ) space (dielectric of 1.0 and AMBER force field). Minima are listed in Table 4.

TABLE 3 Energy minima of **1** in the (χ,γ) conformational space (Fig. 3; ϵ = 4; AMBER94)

Minimum Number	γ (deg)	χ (deg)	Relative Energy (kcal/mol)
1	50.0	−140.0	0.00
2	−70.0	30.0	3.60
3	160.0	170.0	3.66

TABLE 4 Energy minima of **1** in the (χ,γ) conformational space (Fig. 4; ϵ = 4; AMBER94)

Minimum Number	γ (deg)	χ (deg)	Relative Energy (kcal/mol)
1	−170.0	−140.0	0.00
2	−60.0	−140.0	0.73
3	50.0	−140.0	0.73
4	−170.0	20.0	1.86

Typically, the energy plots calculated with the dielectric of 1.0 tend to demonstrate higher barriers to conformational transitions compared to those calculated with the dielectric of 4.0. This effect is more pronounced for the quantum chemically derived charge model than for the model using bond dipole derived charges. This leads to the suggestion that electrostatic forces play a significant role in the determination of the global and secondary minima, specifically in models employing quantum chemically derived charges. For example, the atoms N3, N2, HN2A, and HN2B have partial atomic charges of −0.81, −1.02, 0.476, and 0.476, respectively, in the ab initio derived model, while the corresponding values are −0.01, −0.68, 0.267, and 0.267 in the bond dipole derived model obtained from the MM2 force field. Interactions involving these atoms with other heteroatoms in the molecule will thus tend to dominate more in the former charge model than in the latter.

It is interesting to note that intramolecular hydrogen bonding interactions are restricted to those formed between the C5′ hydroxyl group and N3 of the purine. The hydrogens of the excocyclic amino group in guanine are located farther from O5′ than required for good hydrogen bonding distances, by virtue of the lack of puckering in the didehydrofuran ring. The energy plots corresponding to the inclusion of an implicit solvation model demonstrate a preference for an extended conformation about C4′-C5′ consistent with increased interaction with an effective solvent environment. In these plots, conformations with *syn* orientation of the guanine are destabilized by >2 kcal/mol relative to those with *anti* orientation of the purine. This may be partly due to the relative crowding of the region around the didehydrofuran by the six-membered ring of the guanine in the *syn* orientation while these two rings are farther apart in the *anti* orientation, leading to greater solvent accessible surface area than in the former case.

How do the results of these calculations compare with the available crystal structure information? The limited x-ray crystallographic studies on D4G (Van Roey and Chu, 1992) demonstrate glycosidic torsions of 71° and 83° in two different geometries with *gauche*$^+$ conformations about C4′-C5′ ($\gamma \sim 54°$ and 48°). While the observed (*anti*, *gauche*$^+$) conformational combination of the glycosidic and C4′-C5′ torsion is not a global minimum in any of the energy plots, it is a secondary minimum in plots calculated with implicit solvation and/or a dielectric of 4.0. While *anti*

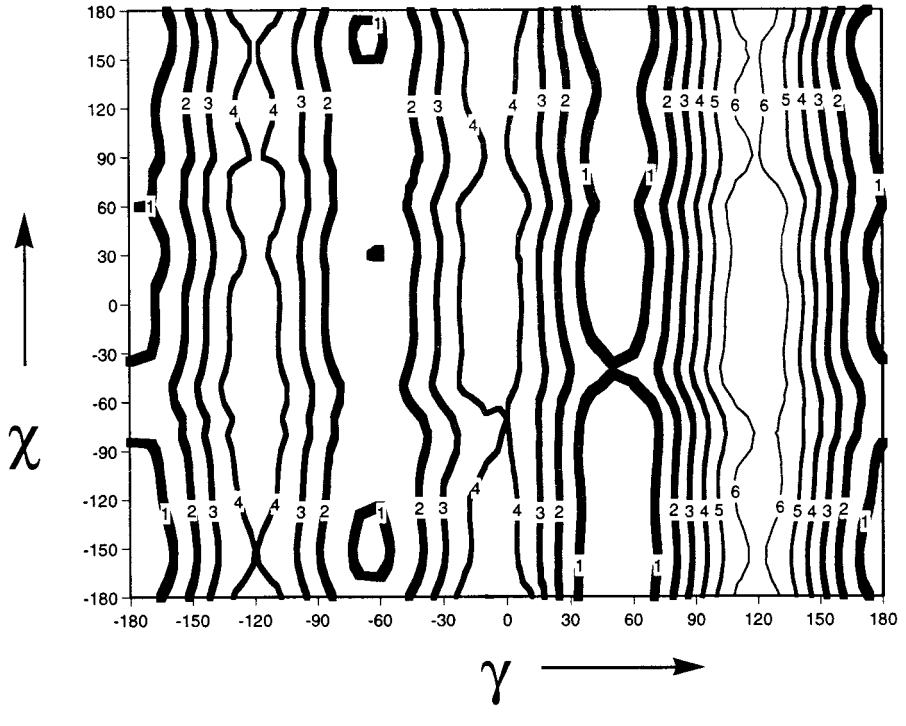

FIGURE 5 Conformational energy map of **1** in the (χ,γ) space (dielectric of 1.0 and MM2 force field with MM2 charges). Minima are listed in Table 5.

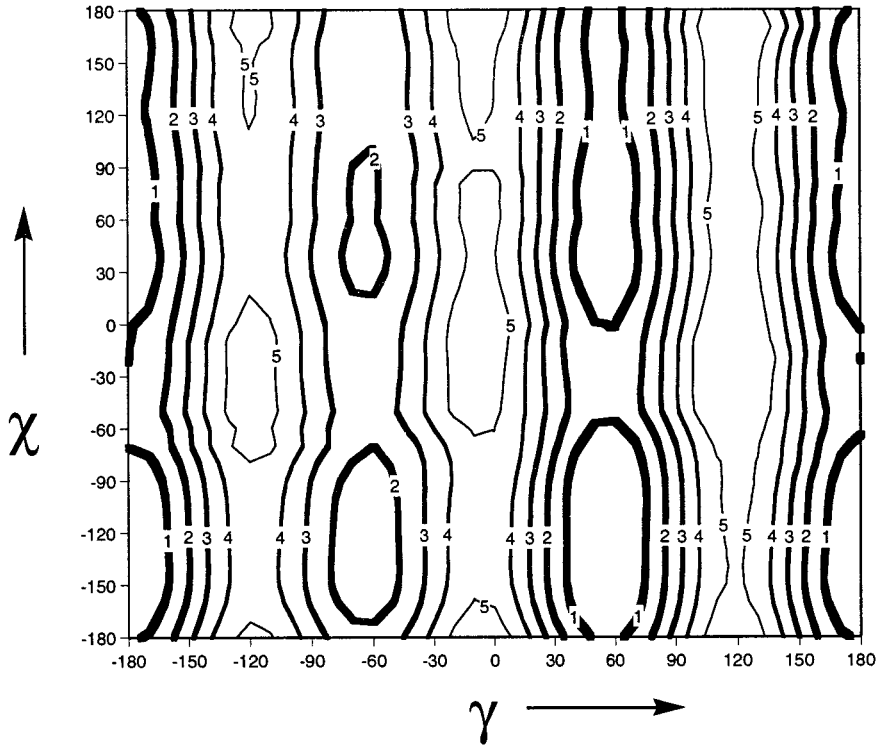

FIGURE 6 Conformational energy map of **1** in the (χ,γ) space (dielectric of 4.0 and MM2 force field with MM2 charges). Minima are listed in Table 6.

orientation of the base is found in global minima of energy plots incorporating the implicit GB/SA solvation approach, these minima demonstrate a *trans* conformation about C4′-C5′. A possible explanation for this discrepancy between the theoretical models and the x-ray data could lie in the intermolecular packing interactions present in the x-ray lattice. Such interactions would be dominated by hydrogen bonding involving the C5′ hydroxyl and the exocyclic amino and carbonyl groups of the guanine base. Since our calculations have been done on a single molecule rather than a lattice, such intermolecular interactions are not explicitly taken into account. On the other hand, additional x-ray studies involving D4G and its analogs are in order to explore the variety of the conformational space accessible to it, as demonstrated through the present calculations.

Comparing the results of the present calculations with corresponding ones on guanine ribo and deoxyribonucleosides, reported previously in the literature (Saenger, 1984), it is found that the unsaturated five-membered ring does not lead to significant variations in the normal conformational preferences about the glycosidic (*syn* and *anti*) and C4′-C5′ bonds (*gauche* and *trans*). However, their conformational combinations in the global minima of the nucleosides with the saturated and unsaturated five-membered rings are different. These preferences are influenced by stronger intramolecular hydrogen bonding (between the exocyclic amino group of the base with O5′) in the saturated compound due to the pseudorotational flexibility of the furanose. These observations imply that D4G and its analogs could be potentially used as surrogates for guanine nucleotides in the design of therapeutic agents (e.g., anticancer drugs with a mechanism of action involving nucleotide recognition).

CONCLUSION

Conformational energy calculations on 2′,3′-dideoxy-2′,3′-didehydroguanidine using a variety of computational protocols encompassing force field, charge and dielectric models indicate that its conformational preferences about the

TABLE 5 Energy minima of **1** in the (χ,γ) conformational space (Fig. 5; ϵ = 1; MM2) using the MM2 charge model

Minimum Number	γ (deg)	χ (deg)	Relative Energy (kcal/mol)
1	50.0	−90.0	0.00
2	180.0	160.0	0.13
3	−60.0	−150.0	0.81
4	−70.0	160.0	0.90

TABLE 6 Energy minima of **1** in the (χ,γ) conformational space (Fig. 6; ϵ = 4; MM2) using the MM2 charge model

Minimum Number	γ (deg)	χ (deg)	Relative Energy (kcal/mol)
1	60.0	−100.0	0.00
2	180.0	−140.0	0.11
3	−60.0	−140.0	1.46
4	−60.0	40.0	1.72

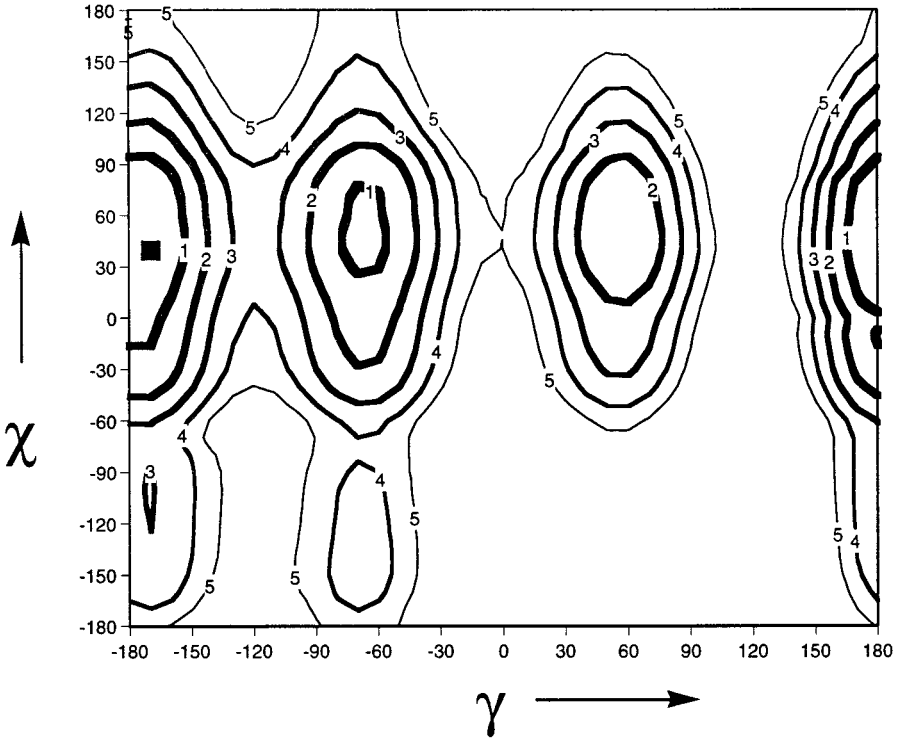

FIGURE 7 Conformational energy map of **1** in the (χ,γ) space (dielectric of 1.0, ab initio charges, and MM2 force field with GBSA solvation model). Minima are listed in Table 7.

glycosidic and C4′-C5 bonds are very sensitive to the protocol employed. The energy profiles in the (χ,γ) conformational energy plots of this compound are generally similar to those of the corresponding nucleoside with a flexible furanose only when the calculations are done with a higher dielectric constant, independent of the charge model used. The observed x-ray data on D4G-containing systems are limited and the glycosidic orientations therein are again

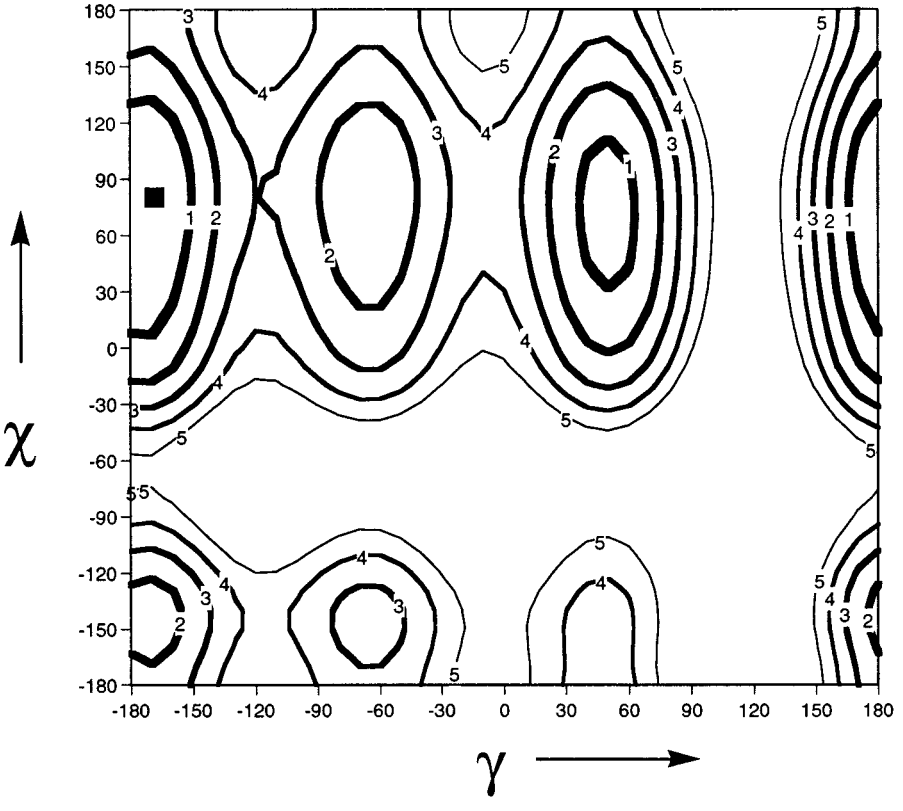

FIGURE 8 Conformational energy map of **1** in the (χ,γ) space (dielectric of 1.0, ab initio charges, and AMBER94 force field with GBSA solvation model). Minima are listed in Table 8.

TABLE 7 Energy minima of **1** in the (χ,γ) conformational space (Fig. 7; $\epsilon = 1$; MM2) using the GB/SA solvation model in conjunction with ab initio charges

Minimum Number	γ (deg)	χ (deg)	Relative Energy (kcal/mol)
1	−170.0	40.0	0.00
2	−70.0	50.0	0.75
3	60.0	50.0	1.03
4	−70.0	−140.0	3.53

TABLE 8 Energy minima of **1** in the (χ,γ) conformational space (Fig. 8; $\epsilon = 1$; AMBER94) using the GB/SA solvation model in conjunction with ab initio charges

Minimum Number	γ (deg)	χ (deg)	Relative Energy (kcal/mol)
1	−170.0	80.0	0.00
2	50.0	70.0	0.61
3	−60.0	80.0	1.27
4	−170.0	−140.0	1.48
5	−70.0	−150.0	2.56

APPENDIX Atom names and their partial atomic charges on **1** (in atomic units) calculated by fitting to the ab initio electrostatic potential surface obtained by using the 6-31G* basis set (ESP) and derived from bond dipoles in the MM2 force field (MM2)

Atom	ESP	MM2
O5′	−0.654	−0.310
HO5′	0.414	0.246
C5′	0.074	0.065
H5′A	0.034	0.0
H5′B	0.021	0.0
C4′	0.656	0.107
H4′	−0.029	0.0
O1′	−0.580	−0.130
C1′	0.445	0.320
H1′	0.083	0.0
N9	−0.033	−0.526
C8	0.172	0.252
H8	0.144	0.0
N7	−0.590	−0.252
C5	0.117	0.157
C6	0.674	0.479
O6	−0.590	−0.479
N1	−0.779	−0.267
H1	0.433	0.267
C2	0.992	0.157
N2	−1.057	−0.690
H2NA	0.476	0.267
H2NB	0.476	0.267
N3	−0.810	−0.010
C4	0.183	0.157
C2′	−0.359	−0.042
H2′	0.224	0.0
C3′	−0.364	−0.042
H3′	0.215	0.0

consistent with either a higher dielectric model or an implicit solvation included model.

REFERENCES

Andrei, G., R. Snoeck, J. Balzarini, and E. De Clercq. 1995. Combination of azidothymidine (AZT) and (E)-5-(2-bromovinyl)-2′-deoxyuridine (BVDU) inhibits the replication of herpes simplex virus type 1 (HSV-1) and type 2 (HSV-2) and varicella zoster virus (VZV) strains that are deficient in the expression of the viral thymidine kinase (TK). *Nucleosides Nucleotides*. 14:559–562.

Bhattacharya, B. K., J. O. Ojwang, R. F. Rando, J. H. Huffman, and G. R. Revankar. 1995. Synthesis and anti-DNA viral activities in vitro of certain 2,4-disubstituted-7-(2-deoxy-2-fluoro-β-D-arabinofuranosyl)pyrrolo[2,3-d]pyrimidine nucleosides. *J. Med. Chem.* 38:3957–3966.

Bolon, P. J., P. Wang, C. K. Chu, G. Gosselin, V. Boudou, C. Piera, C. Mathe, J.-L. Imbach, A. Faraj, M. A. El Alaoui, J.-P. Sommadossi, S. B. Pai, Y.-L. Zhu, J.-S. Lin, Y.-C. Cheng, and R. F. Schinazi. 1996. Anti-human immunodeficiency and anti-hepatitis B virus activities of β-L-2′,3′-dideoxy purine nucleosides. *Bioorg. Med. Chem. Lett.* 6:1657–1662.

Chu, C. K., V. S. Bhadti, B. Doboszewski, Z. P. Gu, Y. Kosugi, K. C. Pullaiah, and P. Van Roey. 1989. General syntheses of 2′,3′-dideoxynucleosides and 2′,3′-didehydro-2′,3′-dideoxynucleosides. *J. Org. Chem.* 54:2217–2225.

Chu, C. K., R. F. Schinazi, B. H. Arnold, D. L. Cannon, B. Doboszewski, V. B. Bhadti, and Z. Gu. 1988. Comparative activity of 2′,3′-saturated and unsaturated pyrimidine and purine nucleosides against human immunodeficiency virus type 1 in peripheral blood mononuclear cells. *Biochem. Pharmacol.* 37:3543–3548.

Cody, V., and T. I. Kalman. 1992. Conformational analysis of two anti-HIV nucleoside analogs 2′,3′-dideoxy-3′-fluorocytidine and its N4-dimethylaminomethylene prodrug derivative. *Nucleosides Nucleotides*. 11:731–738.

Cornell, W. D., P. Cieplak, C. I. Bayly, I. R. Gould, K. Merz, D. M. Ferguson, D. C. Spellmeyer, T. Fox, J. W. Caldwell, and P. A. Kollman. 1995. A second-generation force field for the simulation of proteins, nucleic acids, and organic molecules. *J. Am. Chem. Soc.* 117: 5179–5197.

Dyatkina, N., A. Arzumanov, A. Krayevsky, B. O'Hara, Y. Gluzman, P. Baron, C. MacLow, and B. Polsky. 1994. Synthesis and antiviral activity of some fluorinated nucleotide derivatives. *Nucleosides Nucleotides*. 13:325–337.

Eriksson, S., B. Kierdaszuk, B. Munch-Petersen, B. Oeberg, and N. G. Johansson. 1991. Comparison of the substrate specificities of human thymidine kinase 1 and 2 and deoxycytidine kinase toward antiviral and cytostatic nucleoside analogs. *Biochem. Biophys. Res. Commun.* 176: 586–592.

Everaert, D. H., O. M. Peeters, C. J. De Ranter, N. M. Blaton, A. van Aerschot, and P. Herdewijn. 1993a. Conformational analysis of substituent effects on the sugar puckering mode and the anti-HIV activity of 2′,3′-dideoxypyrimidine nucleosides. *Antiviral Chem. Chemother.* 4:289–299.

Everaert, D. H., and C. J. De Ranter. 1993b. Aqueous molecular dynamics simulations of eight modified 2′,3′-dideoxypyrimidine nucleosides. *J. Am. Chem. Soc.* 115:11209–11212.

Frisch, M. J., G. W. Trucks, H. B. Schlege, P. M. W. Gill, B. G. Johnson, M. A. Robb, J. R. Cheeseman, T. Keith, G. A. Petersson, J. A. Montgomery, K. Raghavachari, M. A. Al-Laham, V. G. Zakrzewski, J. V. Ortiz, J. B. Foresman, J. Cioslowski, B. B. Stefanov, A. Nanayakkara, M. Challacombe, C. Y. Peng, P. Y. Ayala, W. Chen, M. W. Wong, J. L. Andres, E. S. Replogle, R. Gomperts, R. L. Martin, D. J. Fox, J. S. Binkley, D. J. Defrees, J. Baker, J. P. Stewart, M. Head-Gordon, C. Gonzalez, and J. A. Pople. 1995. Gaussian 94, Revision D.3. Gaussian, Inc., Pittsburgh PA.

Galisteo, D., J. A. L. Sastre, and H. Martinez-Garcia. 1996. Conformational comparative analysis of pyrimidine nucleoside derivatives by molecular mechanics calculations and by semiempirical methods (AM1). *J. Mol. Struct.* 384:25–33.

Galisteo, D., J. A. L. Sastre, H. M. Garcia, and R. N. Miguel. 1995. Conformational comparative analysis of 2′,3′-dideoxythymidine ana-

logs by molecular mechanics calculations (CHEM-X) and by semiempirical methods (AM1). *J. Mol. Struct.* 350:147–160.

Genu-Dellac, C., G. Gosselin, A. M. Aubertin, G. Obert, A. Kirn, and J. L. Imbach. 1991. 3′-Substituted thymine α-L-nucleoside derivatives as potential antiviral agents: synthesis and biological evaluation. *Antiviral Chem.* 2:83–92.

Harte, W. E., Jr., J. E. Starrett, Jr., J. C. Martin, and M. M. Mansuri. 1991. Structural studies of the anti-HIV agent 2′,3′-didehydro-2′,3′-dideoxythymidine (D4T). *Biochem. Biophys. Res. Commun.* 175: 298–304.

Herdewijn, P., J. Balzarini, M. Baba, R. Pauwels, A. Van Aerschot, G. Janssen, and E. De Clercq. 1988. Synthesis and anti-HIV activity of different sugar-modified pyrimidine and purine nucleosides. *J. Med. Chem.* 31:2040–2048.

Hitchcock, M. J. M. 1991. 2′,3′-Didehydro-2′,3′-dideoxythymidine (D4T), an anti-HIV agent. *Antiviral Chem.* 2:125–132.

McGuigan, C., D. Cahard, H. M. Sheeka, E. De Clercq, and J. Balzarini. 1996a. Phosphoramidate derivatives of d4T with improved anti-HIV efficacy retain full activity in thymidine kinase-deficient cells. *Bioorg. Med. Chem. Lett.* 6:1183–1186.

McGuigan, C., D. Cahard, H. M. Sheeka, E. De Clercq, and J. Balzarini. 1996b. Aryl phosphoramidate derivatives of d4T have improved anti-HIV efficacy in tissue culture and may act by an entirely new mechanism of reverse transcriptase inhibition. *J. Med. Chem.* 39:1748–1753.

Mohamadi, F., N. G. J. Richards, W. C. Guida, R. Liskamp, M. Lipton, C. Caufield, G. Chang, T. Hendrickson, and W. C. Still. 1990. MacroModel—an integrated software system for modeling organic and bioorganic molecules using molecular mechanics. *J. Comp. Chem.* 11: 440–467.

O'Leary, D. J., and Y. Kishi. 1994. Preferred conformation of C-glycosides. 13. A comparison of the conformational behavior of several C-, N-, and O-furanosides. *J. Org. Chem.* 59:6629–6636.

Rao, S. N. 1995. Conformational studies on deoxyribonucleosides of C6-substituted pyrimidines. *Nucleosides Nucleotides*. 14:1179–1193.

Rao, S. N. 1998. Conformational studies on nucleosides with furanose ring modifications. 1. *Nucleosides Nucleotides*. 17:791–814.

Robins, M. J., J. S. Wilson, D. Madej, N. H. Low, F. Hansske, and S. F. Wnuk. 1995. Nucleic acid related compounds. 88. Efficient conversions of ribonucleosides into their 2′,3′-anhydro, 2′ (and 3′)-deoxy, 2′,3′-didehydro-2′,3′-dideoxy, and 2′,3′-dideoxynucleoside analogs. *J. Org. Chem.* 60:7902–7908.

Russell, J. W., V. J. Whiterock, D. Marrero, and L. J. Klunk. 1989. Pharmacokinetics of a new anti-HIV agent: 2′,3′-dideoxy-2′,3′-didehydrothymidine (d4T). *Nucleosides Nucleotides*. 8:845–848.

Saenger, W. 1984. Principles of Nucleic Acid Structure. Springer, New York. 105–200.

Smee, D. F., H. A. Alaghamandan, K. Ramasamy, and G. R. Revankar. 1995. Broad-spectrum activity of 8-chloro-7-deazaguanosine against RNA virus infections in mice and rats. *Antiviral Res.* 26:203–209.

Van Roey, P., and C. K. Chu. 1992. The crystal and molecular structure of the complex of 2′,3′-didehydro-2′,3′-dideoxyguanosine with pyridine. *Nucleosides Nucleotides*. 11:1229–1239.

Van Roey, P., E. W. Taylor, C. K. Chu, and R. F. Schinazi. 1993. Conformational analysis of 2′,3′-didehydro-2′,3′-dideoxypyrimidine nucleosides. *J. Am. Chem. Soc.* 115:5365–5371.